ACS APPLIED MATERIALS & INTERFACES

Research Article

www.acsami.org

Transfer of Ultrasmall Iron Oxide Nanoparticles from Human Brain-Derived Endothelial Cells to Human Glioblastoma Cells

Blanka Halamoda Kenzaoui,[†] Silvia Angeloni,*[,‡] Thomas Overstolz,[‡] Philippe Niedermann,[‡] Catherine Chapuis Bernasconi,[†] Martha Liley,[‡] and Lucienne Juillerat-Jeanneret*[,†]

[†]Centre Hospitalier Universitaire Vaudois (CHUV) and University of Lausanne (UNIL), Lausanne, Switzerland

[‡]Centre Suisse d'Electronique et de Microtechnique, CSEM SA, Neuchâtel, Switzerland

ABSTRACT: Nanoparticles (NPs) are being used or explored for the development of biomedical applications in diagnosis and therapy, including imaging and drug delivery. Therefore, reliable tools are needed to study the behavior of NPs in biological environment, in particular the transport of NPs across biological barriers, including the blood–brain tumor barrier (BBTB), a challenging question. Previous studies have addressed the translocation of NPs of various compositions across cell layers, mostly using only one type of cells. Using a coculture model of the human BBTB, consisting in human cerebral endothelial cells preloaded with ultrasmall superparamagnetic iron oxide nanoparticles (USPIO NPs) and unloaded human glioblastoma cells grown on each side of newly developed ultrathin permeable silicon nitride supports as a model of the human BBTB, we demonstrate for the first time the transfer of USPIO NPs from human brain-derived endothelial cells to glioblastoma cells. The reduced thickness of the permeable mechanical support compares better than commercially available polymeric supports to the thickness of the basement membrane of the cerebral vascular system. These results are the first report supporting the possibility that USPIO NPs could be directly transferred from endothelial cells to glioblastoma cells across a BBTB. Thus, the use of such ultrathin porous supports provides a new in vitro approach to study the delivery of nanotherapeutics to brain cancers. Our results also suggest a novel possibility for nanoparticles to deliver therapeutics to the brain using endothelial to neural cells transfer.

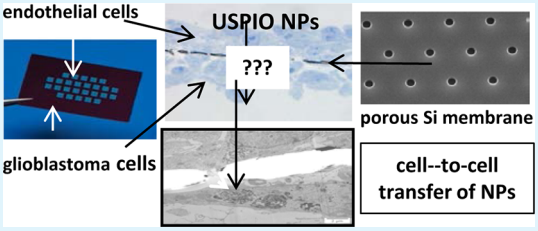

KEYWORDS: *nanoparticles, cell–cell transfer, porous ultrathin silicon nitride membrane, human blood–brain tumor barrier, therapeutics delivery*

1. INTRODUCTION

Nanotechnology has brought a variety of new possibilities into medicine, ranging from diagnosis of diseases to novel therapies.[1−3] Strategies to improve the delivery of therapeutics to the brain tissue without opening of the brain vascular system are urgently needed. Nanocarriers and nanovectors, including nanoparticles, are a valid opportunity to achieve this goal, in particular in brain cancers. Such an achievement would involve the transport of the nanoparticulate therapeutics, from the luminal to the basolateral sides of the brain vascular system across the endothelial cells, if such a transport system can be designed. Ultrasmall superparamagnetic iron oxide nanoparticles (USPIO NPs) are particularly promising devices since their magnetic properties increase the number of possible applications in many areas of the biomedical field, including drug delivery, thermotherapy, imaging and detection of cancer.[4,5] However, their potential and pathways to cross biological barriers, including the blood–brain barrier (BBB) and the blood–brain tumor barrier (BBTB) needs to be confirmed if they are to be used in the diagnosis and therapy of brain diseases and brain tumors.[6−8] Previous studies, including ours, have addressed the translocation of NPs of various compositions across cell layers using two-compartments devices separated by a polymeric membrane, but these previous studies have used only one type of cells and did not demonstrate a very efficient transport, possibly because of the characteristics of the polymeric membrane separating the two compartments.[9−13] Only one previous study[14] has suggested, using a three-cell coculture model of the lung including epithelial cells, macrophages and dendritic cells, that macrophages and dendritic cells can exchange 1 μm polystyrene NPs via cell extended cytoplasmic processes across the epithelial layer. However, these cells belong to the immune phagocytic lineage and the mechanisms involved need to be defined. Much less information exists concerning the translocation of NPs from the luminal to the basolateral compartments of the vascular wall, in particular in the brain across the BBB in the normal brain, or across the disturbed BBB in diseases of the brain, including the BBTB of brain cancers. Using an immortalized murine brain endothelial cell line, it has very recently been shown that the endothelial layer crossing of fluorescent 100 nm cationic polystyrene NPs was enhanced when derivatized with a cell-penetrating peptide, likely by transcytosis.[13]

Glioblastoma (grade IV astrocytoma) is the most aggressive neoplasm of the central nervous system and is highly resistant to therapy, in part due to poor drug delivery across the BBTB.

Received: December 20, 2012
Accepted: April 11, 2013
Published: April 11, 2013

Glioblastoma neo-vasculature consists of multilayered mitotically active endothelial cells, representing the BBTB. Thus the direct transfer of therapeutics from the endothelial cells of the BBTB to the tumor cells may present a therapeutic advantage. Our previous studies have shown that USPIO NPs are internalized by human HCEC brain-derived endothelial cells, but they were neither released by the cells following uptake, nor transported by HCEC cell layers,[9] across thick polyester membranes. But the results suggested the possible transfer of the NPs by the endothelial cell filopodia to the brain parenchyma.[9]

In the present report, we describe new ultrathin porous silicon nitride supports, made using standard micro fabrication techniques, together with dedicated holders that make them compatible with commercial cell culture well-plates. The resulting setup allows for interaction between the upper and lower side of the permeable support, providing a new tool to study the transport of NPs in vitro, more representative of the in vivo situation. To develop a model of the BBTB, human cerebral endothelial cells (HCEC) preloaded with uncoated USPIO NPs which are highly internalized by HCEC cells,[9] were layered on one side of the porous silicon nitride support and USPIO NPs-unloaded LN229 human glioblastoma cells were layered on the other side of the same support. Then, this model was used to evaluate whether a direct transfer of the USPIO NPs from endothelial cells to glioblastoma cells could be demonstrated.

2. EXPERIMENTAL SECTION

2.1. Preparation of Silicon Nitride Porous Supports. The supports for cell growth and evaluation of the transfer of NPs were made of low stress silicon nitride (Si_3N_4, enriched in silicon, i.e., Si_xN_y with $x > 3$ and $y < 4$ compared to the stoichiometric Si_3N_4). They were fabricated using standard microfabrication technology.[15−19] Briefly, a 500 nm thick layer of low stress silicon nitride was deposited on both sides of a 380 μm thick silicon wafer (Siltronix SAS, France) by low pressure chemical vapor deposition (LPCVD), in a dedicated oven where the silicon-rich silicon nitride is formed by a gas flow of dichlorosilane (SiH_2Cl_2) in presence of ammonia (NH_3) (SiH_2Cl_2 and NH_3 from Carbagas, Gümligen, CH). The thickness and homogeneity of the deposited silicon nitride were measured at several spots using a NanoCalc 2000 white light interferometer (Ocean Optics Inc., USA). Standard photolithography and reactive ion etching (RIE) were used to pattern the silicon nitride on both sides of the wafer. The pattern on the bottom side defined the pore size, pore shape, and the arrangement of the pores in the silicon nitride layer. These features were inspected by scanning electron microscope (SEM XL 40 Philips, Nederland). On the top of the wafer, square openings of 1.70 mm × 1.70 mm were etched into the silicon nitride. In the subsequent step—an anisotropic chemical etching in potassium hydroxide (KOH) solution—the silicon nitride protected the silicon from being etched, while the square openings in the silicon nitride resulted in pyramidal pits (microwells) etched into the silicon wafer. The anisotropic etching was stopped once the pyramidal pits went through the whole wafer such that an array of freestanding silicon nitride porous windows (each 1160 μm × 1160 μm, and displaying 2 μm pores) were formed. The wafer was coated with photoresist in order to protect the fragile porous window array during dicing of the wafer into individual chips. The photoresist on the diced chips was removed in acetone and isopropanol prior to cleaning the chips in hot Piranha solution (98% H_2SO_4:30% H_2O_2 4:1, at 110 °C), followed by extensive rinsing with deionized water and drying under laminar flow. The array of porous silicon nitride windows is mechanically supported by the surrounding silicon chip, which will be referred to in the following text as silicon nitride porous supports or ceramic chips or ceramic substrates, emphasizing the silicon nitride interface that is in contact with the cell lines object of this study. Specially designed plastic holders allowed the use of the ceramic porous supports in standard six-well cell culture plates.

2.2. Pretreatment and Regeneration of Silicon Nitride Porous Supports. After fabrication, the porous supports were cleaned with Piranha solution as described above, then stored in clean in Milli-Q water until use. Alternatively, they can be dried and cleaned with SC1 solution ("Standard Clean 1": 24% NH_4OH:30% H_2O_2:deionized water 1:1:5, at 70 °C) followed by extensive rinsing with water and drying at room temperature immediately prior to use. For cell culture use, the devices were immersed in cell culture medium for at least 30 min before cell seeding. After completion of the cell experiments the devices can be cleaned using Piranha solution and reused.

2.3. USPIO NPs. Uncoated iron oxide nanoparticles (Fe_3O_4, uncoated USPIO NPs) were obtained from PlasmaChem (PlasmaChem GmbH Adlershof, Germany) as a ∼3% nanosuspension in water, 18 mg/mL of iron as determined by the Prussian Blue reaction, average nanoparticle size 8 ± 3 nm (as determined by dynamic light scattering (DLS) by the provider), zeta potential −3 mV (pH 7, value provided by D. Bilanicova, University of Venice), +15 mV in 10 mM NaCl, −25 mV in DMEM (values provided by the provider), as previously described.[9]

2.4. Cell Lines and Culture Conditions, Cell Viability, and DNA Synthesis. Human HCEC brain-derived endothelial cells (a kind gift from D. Stanimirovic, Ottawa, Canada) and human LN229 glioblastoma cells (American Type Culture Collection, ATCC, Manassas, VA) were grown in DMEM medium, containing 4.5 g/L glucose, 10% FCS and penicillin/streptomycin antibiotics (Gibco, Invitrogen, Basel, Switzerland). For cell viability and DNA synthesis, cells were grown in 48-well cell culture plates (Costar, Corning, NY, USA) until 75% confluent and exposed to the USPIO NPs in complete culture medium for the concentration and time indicated, then washed in saline (0.9% NaCl (w/v)). Cell viability was evaluated using the MTT assay, essentially as previously described.[9] DNA synthesis was determined by tritiated thymidine (^{3}H-T) incorporation, essentially as previously described.[9] Then, the absorbance readings or the radioactivity counts of treated cells were compared to the absorbance readings or the radioactivity counts, respectively, of untreated cells. All experiments were performed in triplicate wells, and repeated at least twice. Means ± standard deviations (sd) were calculated.

2.5. Cell Uptake of USPIO NPs. Cells were grown in 48-well plates until 75% confluent, then exposed to the USPIO NPs for the concentration and time indicated. Then, cell-associated iron content was quantified by the soluble Prussian Blue reaction, essentially as previously described.[9] Briefly, for quantitative iron determination, the cell layers were dissolved in 6 N HCl, then a 5% solution of $K_4[Fe(CN)_6]\cdot 3H_2O$ (Merck, VWR international, Nyon, Switzerland) in H_2O was added for 10 min and the absorbance was measured at 690 nm in a multiwell plate reader (iEMS Labsystems). A standard curve of $FeCl_3$ in 6 N HCl treated under the same conditions was used to quantify the amount of cell-bound iron. All experiments were performed in triplicate wells, and repeated at least twice. Means ± sd were calculated.

2.6. Endothelium−Glioblastoma Barrier Model. Silicon nitride porous supports placed in the dedicated plastic holders were inserted into wells of a six-well cell culture plate (Costar) and immersed in complete culture medium for 30 min. Then, after removal of the culture medium, 200 μL of LN229 cell suspension (8×10^5 cells/mL) were added to the side of the chip displaying the open, etched face of the porous pyramidal microwells ("top side" of the chip) and incubated in a humidified cell culture incubator at 37 °C, top side up for 3 days. Then, when the cells strongly adhered and ∼80% confluent, the porous supports were transferred into new wells of a six-well plate with fresh medium, top side down, and 200 μL of HCEC cells (3×10^6 cells/mL), preloaded with USPIO NPs (50 μg/mL) for 24 h, detached with trypsin-EDTA (trypsin-versene, Gibco) and washed 3 times with PBS by centrifugation, was added to the flat bottom side of the porous supports. The coculture system was incubated at 37 °C in a

humidified cell culture incubator for 3 days, and analyzed by microscopy techniques.

Alternatively, for the visualization of the iron core associated with the cells, the histochemical determination of iron in the cell layers was also performed. After coculture on the silicon nitride porous supports the cell layers were washed with PBS and detached with trypsin-EDTA, first HCEC cells, then LN229 cells, collected separately, centrifuged, and seeded on microscope glass slides (4-chambers Polystyrene Vessel Culture Slides, BD Falcon, Erembodegem, Belgium) and cultured separately for 24 h, then cell-associated iron was determined using the histological Prussian Blue technique. The cell layers were washed in PBS, fixed in 4% buffered paraformaldehyde for 3 h at 4 °C and incubated for 20 min at room temperature with a 1:1 solution of 10% HCl and 5% $K_4[Fe(CN)_6]\cdot 3H_2O$ in H_2O, washed with distilled water, counterstained with Nuclear Fast Red, dehydrated in graded ethanol to xylol, and mounted. Slides were photographed under a Nikon digital camera (DXM 1200; Nikon Corporation, Tokyo, Japan). Then the number of blue iron spots per cell was counted in 5 different fields of the recultures and averaged per cell ± sd.

2.7. Transmission Electron Microscopy (TEM) and Light Microscopy (semithin cuts). The porous silicon nitride supports with the HCEC cell layers on one side and the LN229 cell layers on the other side were washed in PBS and fixed in 3% glutaraldehyde (Sigma) in PBS for 24 h. Then they were washed in 0.2 M cacodylate, postfixed in 1.3% osmium tetroxide in 0.2 M cacodylate for 1 h and dehydrated in graded ethanol, then in propylene oxide, and embedded in Epon (50% (w/w) Epon 812 substitute, 26% (w/w) dodecenyl-succinic anhydride (DDSA), 23% (w/w) methylnadic anhydride (MNA), 1% (w/w) 2,4,6-tris(dimethylaminomethyl)phenol (DMP-30)) (all from Fluka). Blocks were cured for 48 h at 60 °C, then thin (500 nm for light microscopy) and ultrathin sections (90 nm for TEM), respectively, were cut using an ultramicrotome (Ultracut E, Reichert-Jung Optische Werke AG, Wien, Austria). For light microscopy the slides were stained using methylene blue/azure histological staining and mounted. For TEM examination, slides were mounted on 3 mm 200-mesh copper grids. Grids were stained for 75 min in saturated uranyl acetate (Fluka) solution, then for 100 s in lead citrate (Ultrostain 2, Lavrylab). They were then examined and photographed at 80 kV with a Philips CM10 TEM combined with a MegaView III Soft Imaging system.

3. RESULTS AND DISCUSSION

We have previously shown that functionalized USPIO NPs, either positively charged and drug-derivatized or unfunctionalized uncoated (bare) USPIO NPs are easily and at high level taken up by human cells of different tissue origin, including brain-derived endothelial cells, but are not transported across cell layers.[20−24] Understanding the possibility for therapeutics to cross biological barriers and penetrate tissues is fundamental for evaluating their therapeutic potential for human diseases.[25,26] The treatment of tumors of the central nervous system (CNS) is challenging, as it requires the overcoming of the BBTB which prevents the cerebral accumulation of a pharmacologically sufficient amount of therapeutics. Nanotechnologies may provide possible solutions to this challenge.[27,28] The efficiency of the transport of nanotherapeutics to the CNS is generally evaluated in vivo using animal models,[29,30] although the reliability of the results when transposed into human remains uncertain. Various ex vivo models established for the investigation of drug transport across the BBB are also employed to study nanoparticulate systems.[31−33] However, the porous polyester filters developed for the transport of small molecules are not optimal for USPIO NPs, because their thickness and pores not aligned to the surface of the membrane limit the passage of the NPs. In order to overcome this problem, we developed ultrathin porous silicon nitride supports and evaluated the transfer of USPIO NPs from human cerebral endothelial cells to human glioblastoma tumor cells across this ultrathin membrane permeable to the NPs. In the present report, we focused on unfunctionalized uncoated (bare) USPIO NPs that are easily accessible and commercially available.

The porous silicon nitride cell culture supports are rectangular hard ceramic chips (14 mm × 23 mm) each with an array of 26 square microwells, having a depth of 381 μm and a surface area of 1.35 mm^2 (Figure 1A, C). Specially designed

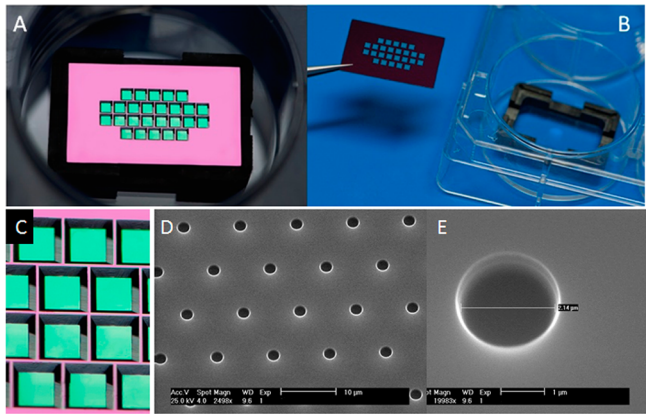

Figure 1. Ultrathin porous silicon nitride support. (A) Macrostructure of the silicon nitride porous support (14 × 23 mm). The ultrathin porous surface is distributed over the 26 microwells arranged in 4 rows. (B) For cell culture, the silicon nitride porous support is inserted into a holder adapted to a well of a six-well plate. (C) Close up of the array of the silicon nitride microwells (381 μm deep). The bottom edge of a single well is 1160 μm long and the porous area is 1.35 mm^2. (D) SEM image of the porous silicon nitride layer showing pores of 2 μm diameter. Adjacent pores of the hexagonal pattern are 7.1 μm apart of each other according to 10% filling factor. (E) SEM image of a single pore 2.14 μm in diameter.

plastic holders (Figure 1B) hold the individual ceramic chips and can be placed in standard six-well cell culture plates. The structures on the bottom side define the pore size, pore shape, and the period of the pores in the porous support itself. On the other side of the wafer, square openings of 1.7 mm × 1.7 mm are present (Figure 1C). Scanning electron microscopy (SEM) images of the porous silicon nitride sheets, 500 nm thick, demonstrated the presence of perfectly ordered 2 μm pores according to a 5 or 10% filling factor (Figure 1D, E). Each chip features 35.1 mm^2 of porous surface, with periodically distributed 2 μm holes with cylindrical walls (Figure 1E) 500 nm high, which corresponds to the surface occupied by the pyramidal microwell porous bottom layers (edge 1.16 mm). The same surface is available for the cell growth on the opposite side of the support for the cocultures of the cells.

First we quantified the uptake of NPs by HCEC cells using the soluble quantitative Prussian Blue reaction (Figure 2A). The results showed that HCEC cells take up high amounts of uncoated USPIO NPs confirming previous results.[9] In these cells, this uptake decreased the cell metabolic activity[9,34] and their synthesis of DNA (Figure 2B), but only at the highest concentrations of USPIO NPs. The internalization into cell organelles of USPIO NPs by HCEC cells was confirmed by TEM, without evidence of the presence of the NPs at the surface of the HCEC cell membrane (Figure 2C). The uptake of USPIO NPs by LN229 cells increased dose-dependently,

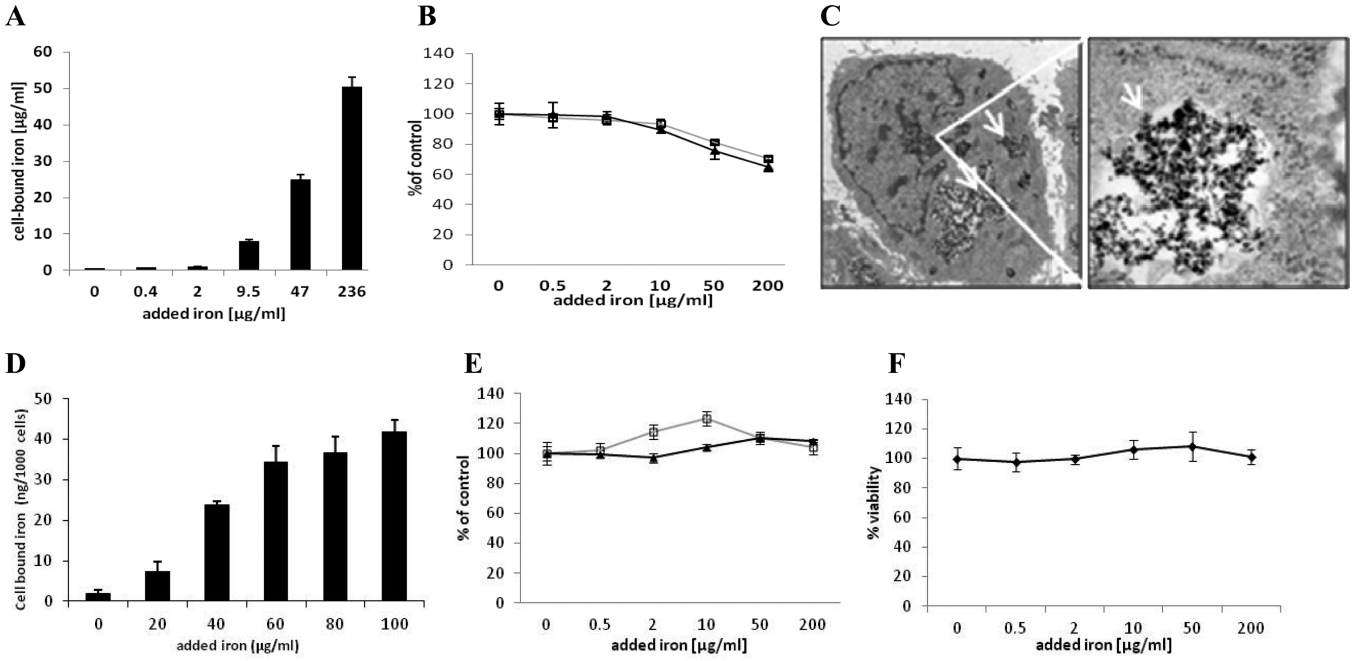

Figure 2. Uptake by and cytotoxicity of USPIO NPs for LN229 cells and HCEC cells. (A). Uptake of USPIO NPs quantified as cell-associated iron in HCEC cells exposed for 24 h to USPIO NPs. (B) Synthesis of DNA by HCEC cells exposed for 24 h (gray curve) or 48 h (black curve) to USPIO NPs. (C) TEM images of HCEC cells exposed for 24 h to USPIO NPs. The NPS localized in intracellular NPs clusters (white arrows) and are not detected at the cell surface. (D) Uptake of USPIO NPs quantified as cell-associated iron in LN229 cells exposed for 24h to USPIO NPs. (E) DNA synthesis after 24 h (gray curve) or 48 h (black curve) exposure of LN229 cells to USPIO NPs. (F) Cell metabolic activity and survival after 72 h exposure of LN229 cells to USPIO NPs.

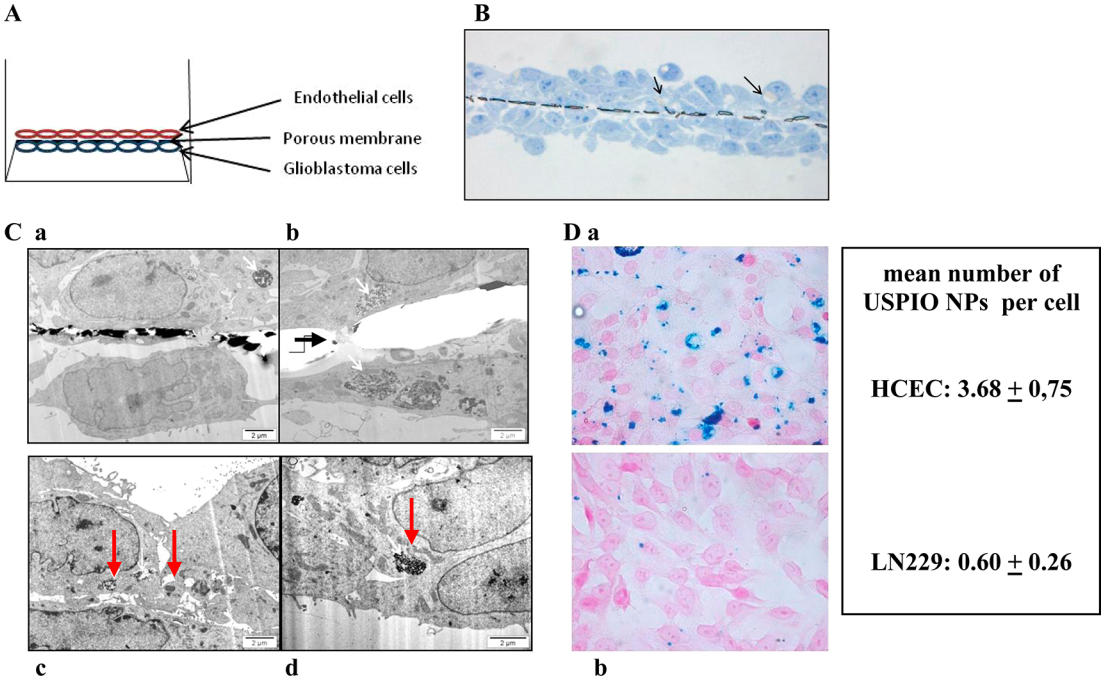

Figure 3. Transfer of USPIO NPs from HCEC cells to LN229 cells across the silicon nitride membrane. (A) Schema of the experimental setup. (B) USPIO NPs-preloaded HCEC cells and unloaded LN229 cells after 3 days of coculture on each side of the porous silicon nitride porous support (HCEC cells, upper layer; LN229 cells, lower layer), analyzed by light microscopy of thin sections. The porous support shatters during histological and sample preparation and appears as a black broken line. NPs clusters are visible in HCEC cells (black arrow) as brown spots. (C) (a) TEM images of ultrathin sections (HCEC cells, upper layer; LN229 cells, lower layer; silicon nitride membrane, black broken line). (b) The pores can be identified by the presence of cellular material bridging the two cell layers (black arrow). Clusters of NPs are also visible in the cells. Higher-magnification images show clusters of NPs (red arrows) visible in (c) HCEC cells and (d) LN229 cells. (D) Following separate reculturing of both cells cell-associated iron was analyzed (HCEC cells, a; LN229 cells, b; iron, blue; nucleus, red; cytoplasm, pink). The aspect of the nuclei and nucleoli (dark pink spots inside the nuclei) in LN229 cells ascertain their tumoral character, compared to HCEC cells. The mean number of USPIO NPs per cell was calculated by counting and averaging the number of iron blue spots per cell in 5 different fields.

dx.doi.org/10.1021/am401310s | ACS Appl. Mater. Interfaces 2013, 5, 3581−3586

with a tendency to saturation for concentrations higher than 60 μg/mL (Figure 2D), comparable to HCEC cells.[9] However, in the LN229 glioblastoma cells, the cell metabolic activity and survival or DNA synthesis were not affected by the USPIO NPs (Figure 2E, F). Therefore uncoated USPIO NPs can be taken up by both cells, without unacceptable cytotoxicity.

We have also previously shown that uncoated USPIO NPs were easily internalized by human brain-derived HCEC endothelial cells, but were not subsequently released or transported by these cells.[9] However, we observed the presence of USPIO NPs loaded filopodia able to invade and cross the polyester filters suggesting the possibility for transferring the NPs from endothelial cells to underlying brain tumor cells. Therefore in the present approach, we tested this possibility using these newly developed ultrathin porous silicon nitride membrane. Prior to seeding, HCEC cells were preloaded for 24h (which we previously demonstrated as an optimal loading time)[9] with the USPIO NPs, then cultured on one side of the porous silicon nitride supports with unloaded LN229 glioblatoma cells on the other side of the membrane (Figure 3A, B) facilitating the contact between the HCEC and LN229 cell layers (Figure 3Ca), but not cell migration across the membrane. As previously shown using thick polyester filter inserts,[9] HCEC cell filopodia were able to pass through the pores of the silicon nitride porous supports (Figure 3Cb, black arrow). TEM images showed that the majority of the clusters of USPIO NPs were still localized in HCEC cells (Figure 3Cc, red arrows), but interestingly, some USPIO NPs were also found in LN229 cells (Figure 3Cd, red arrow). Following 3-day cocultures, HCEC cells and LN229 cells were recultured separately for 1 day, then analyzed for cell-associated iron by iron-histochemistry (Figure 3D). HCEC cells (Figure 3Da) contained a high amount of blue iron complexes, but the presence of iron was also detected in LN229 cells (Figure 3Db). Counting the iron blue spots in 5 different fields allowed evaluaing the efficacy of the transfer of the NPs between the cells: an average of 3.68 ± 0.75 USPIO NPs per cell were detected in HCEC cells and 0.60 ± 0.26 USPIO NPs per cell in LN229 cells, representing around 15% of the content of HCEC cells. Therefore, it can be estimated that a sizable amount of USPIO NPs were transferred from endothelial cells to glioblastoma cells.

Therefore, these experiments demonstrated that USPIO NPs can be transferred from human brain-derived endothelial cells to glioblastoma cells across a model of the BBTB. The model developed with human cerebral endothelial cells cultured on one side (the luminal side) and human glioblastoma cells on the other side (the basolateral side) of this ultrathin silicon nitride porous support as a model of the BBTB, allowing for close interaction between both cell types, is very promising considering the many research studies aiming at the use of NPs for the diagnosis and therapy of brain cancers.[35−37] We did not analyze in detail the mechanisms of this transfer of USPIO NPs between HCEC and LN229 cells, but it would be tempting to propose the involvement of microvesicles (exosomes and/or ectosomes). These biological pathways involve the shedding of cell fragments from cells into their surroundings, then their reuptake by other cells, because the release of microvesicles has been demonstrated for brain endothelial cells.[38] The use of submicrometer thick porous supports to improve the quality of the previously reported in vitro coculture models of the BBB was already utilized to promote cell−cell signaling through both sides of a two compartments setup.[39] The need for robust, extremely thin, and permeable supports still biocompatible, like silicon, has attracted proficiencies in microfabrication of hard materials. The 500 nm thick porous silicon nitride supports that we developed allowed us evidencing the translocation of USPIO NPs through the BBTB. The robustness of the system allowed it to be reused several times. Up to now, no USPIO NPs and only very few NPs have been shown to be efficiently transported in vitro from endothelial to glioma cells.[40,41] Most studies reporting efficient delivery of nanocarriers to the brain were based on animal models,[30,31,42,43] or only indirectly evidenced NP transport by the therapeutic effect of the drug cargo of the NPs.[44]

CONCLUSION

In conclusion, we have developed ultrathin silicon nitride porous supports representing a useful tool to model the BBTB. To develop an experimental model of the BBTB, human glioblastoma cells and human brain-derived endothelial cells were grown on both sides of this newly developed permeable ultrathin silicon nitride ceramic membrane. The membrane highly porous to NPs was convenient to use and the adsorption of serum proteins from the cell culture medium before cell seeding was sufficient to ensure proper cell adhesion, proliferation and confluence. Then the transfer of iron oxide NPs from the endothelial cell to the glioblastoma cells was evaluated. Using this ultrathin porous support, we could demonstrate that USPIO NPs can be translocated from endothelial cells to glioblastoma cells using an in vitro model representative of the endothelial-glioblastoma tumor barrier. Such novel materials can represent new and convenient approaches to evaluate the delivery of nanotheranostics to brain cancers across the BBTB, as well different biological barriers using appropriate cellular models.

AUTHOR INFORMATION

Corresponding Author

*E-mail: lucienne.juillerat@chuv.ch (L.J.); silvia.angeloni@csem.ch (S.A.). Phone: +41 21 314 7173 (L.J.); +41 32 720 5178 (S.A.). Fax: +41 21 314 7115 (L.J.); +41 720 5740 (S.A.).

Notes

The authors declare no competing financial interest.

ACKNOWLEDGMENTS

We acknowledge the support of the staff of the clean room facilities of CSEM's Microsystems Technology Division. This work was supported in part by grants of the Swiss National Scientific Research Foundation (Grant 3152A0-105705).

REFERENCES

(1) Caruthers, S. D.; Wickline, S. A.; Lanza, G. M. *Curr. Opin. Biotechnol.* **2007**, *18*, 26−30.
(2) Singh, S. *J. Nanosc. Nanotech.* **2010**, *10*, 7906−7918.
(3) Heidel, J. D.; Davis, M. E. *Pharm. Res.* **2011**, *28*, 187−199.
(4) Alexiou, C.; Jurgons, R.; Seliger, C.; Iro, H. *J. Nanosci. Nanotechnol.* **2006**, *6*, 2762−2768.
(5) Zhang, C.; Liu, T.; Gao, J.; Su, Y.; Shi, C. *Mini Rev. Med. Chem.* **2010**, *10*, 193−202.
(6) Chertok, B.; Moffat, B. A.; David, A. E.; Yu, F.; Bergemann, C.; Ross, B. D.; Yang, V. C. *Biomaterials* **2008**, *29*, 487−496.
(7) Weinstein, J. S.; Varallyay, C. G.; Dosa, E.; Gahramanov, S.; Hamilton, B.; Rooney, W. D.; Muldoon, L. L.; Neuwelt, E. A. *J. Cereb. Blood Flow Metab.* **2010**, *30*, 15−35.

(8) Silva, A. C.; Oliveira, T. R.; Mamani, J. B.; Malheiros, S. M.; Malavolta, L.; Pavon, L. F.; Sibov, T. T.; Amaro, E.; Tannús, A.; Vidoto, E. L.; Martins, M. J.; Santos, R. S.; Gamarra, L. F. *Int. J. Nanomed.* **2011**, *6*, 591−603.
(9) Halamoda Kenzaoui, B.; Chapuis Bernasconi, C.; Hofmann, H.; L. Juillerat-Jeanneret, L. *Nanomedicine* **2012**, *7*, 39−53.
(10) Halamoda Kenzaoui, B.; Vila, M. R.; Miquel, J. M.; Cengelli, F.; Juillerat-Jeanneret, L. *Int. J. Nanomed.* **2012**, *7*, 1275−1286.
(11) Halamoda Kenzaoui, B.; Chapuis Bernasconi, C.; Juillerat-Jeanneret, L. *Cell Biol. Toxicol.* **2013**, *29*, 39−58.
(12) Faziollahi, F.; Sipos, A.; Kim, Y. H.; Hamm-Alvarez, S. F.; Borok, Z.; Kim, K. J.; Crandall, E. D. *Int. J. Nanomed.* **2011**, *6*, 2849−2857.
(13) Guarnieri, D.; Falanga, A.; Muscetti, O.; Tarallo, R.; Fusco, S.; Galdiero, M.; Galdiero, S.; Netti, P. A. *Small* **2013**, *9*, 853−862.
(14) Blank, F.; Wehrli, M.; Lehmann, A.; Baum, O.; Gehr, P.; von Garnier, C.; Rothen-Rutishauser, B. M. *Immunobiology* **2011**, *216*, 86−95.
(15) Heuberger, A. In *Mikromechanik: Mikrofertigung mit methoden der Halbleitertechnologie*, 1st ed.; Springer-Verlag: Berlin, 1989.
(16) Frühauf, J. In *Shape and Functional Elements of the Bulk Silicon Microtechnique: A Manual of Wet−Etched Silicon Structures*, 1st ed.; Springer-Verlag: Berlin, 2005.
(17) Madou, M. J. In *Fundamentals of Microfabrication: The Science of Miniaturization*, 3rd ed.; Taylor & Francis: London, 2011.
(18) Kuiper, S.; van Rijn, C. J. M.; Nijdam, W.; Elwenspoek, M. C. *J. Membr. Sci.* **1998**, *150*, 1−8.
(19) Harris, S. G.; Shuler, M. *Biotechnol. Bioprocess Eng.* **2003**, *8*, 246−251.
(20) Petri-Fink, A.; Chastellain, M.; Juillerat-Jeanneret, L.; Ferrari, A.; Hofmann, H. *Biomaterials* **2005**, *26*, 639−646.
(21) Hanessian, S.; Grzyb, J. A.; Cengelli, F.; Juillerat-Jeanneret, L. *Bioorg. Med. Chem.* **2008**, *16*, 2921−2931.
(22) Cengelli, F.; Grzyb, J. A.; Montoro, A.; Hofmann, H.; Hanessian, S.; Juillerat-Jeanneret, L. *ChemMedChem* **2009**, *4*, 988−997.
(23) Cengelli, F.; Maysinger, D.; Tschuddi-Monnet, F.; Montet, X.; Corot, C.; Petri-Fink, A.; Hofmann, H.; Juillerat-Jeanneret, L. *J. Pharm. Exp. Therap.* **2006**, *318*, 108−116.
(24) Cengelli, F.; Voinesco, F.; Juillerat-Jeanneret, L. *Nanomedicine* **2010**, *5*, 1075−1087.
(25) Juillerat-Jeanneret, L.; Schmitt, F. *Med. Res. Rev.* **2007**, *27*, 574−590.
(26) Kievit, F. M.; Zhang, M. *Acc. Chem. Res.* **2011**, *44*, 853−862.
(27) Juillerat-Jeanneret, L. *Drug Discovery Today* **2008**, *13*, 1099−1106.
(28) Wohlfart, S.; Gelperina, S.; Kreuter, J. *J. Controlled Release* **2012**, *161*, 264−273.
(29) Sarin, H.; Kanevsky, A. S.; Wu, H.; Brimacombe, K. R.; Fung, S. H.; Sousa, A. A.; Auh, S.; Wilson, C. M.; Aronova, M. A.; Leapman, R. D.; Griffiths, G. L.; Sharma, K. L.; Hall, M. D. *J. Translat. Med.* **2008**, *6*, 80−95.
(30) Ku, S.; Yan, F.; Wang, Y.; Sun, Y.; Yang, N.; Ye, L. *Biochem. Biophys. Res. Commun.* **2010**, *394*, 871−876.
(31) Ribeiro, M. M.; Castanho, M. A.; Serrano, I. *Mini Rev. Med. Chem.* **2010**, *10*, 262−270.
(32) Vernon, H.; Clark, K.; Bressler, J. P. *Methods Mol. Biol.* **2011**, *758*, 153−168.
(33) Wong, H. L.; Wu, X. Y.; Bendayan, R. *Adv. Drug Delivery Rev.* **2012**, *64*, 686−700.
(34) Halamoda Kenzaoui, B.; Chapuis Bernasconi, C.; Guney-Ayra, S.; Juillerat-Jeanneret, L. *Biochem. J.* **2012**, *441*, 813−821.
(35) Meng, X. X.; Wan, J. Q.; Jing, M.; Zhao, S. G.; Cai, W.; Liu, E. Z. *Acta Pharmacol. Sin.* **2007**, *28*, 2019−2026.
(36) Zhang, L.; Yu, F.; Cole, A. J.; Chertok, B.; David, A. E.; Wang, J.; Yang, V. C. *AAPS J.* **2009**, *11*, 693−699.
(37) Kievit, F. M.; Veiseh, O.; Fang, C.; Bhattarai, N.; Lee, D.; Ellenbogen, R. G.; Zhang, M. *ACS Nano* **2010**, *24*, 4587−4594.
(38) Haqqani, A. S.; Delaney, C. E.; Tremblay, T. L.; Sodja, C.; Sandhu, J. K.; Stanimirovic, D. B. *Fluids Barriers CNS* **2013**, *10*, 4.
(39) Harris, M. A. S.; Lepak, L. A.; Hussain, R. J.; Shain, W.; Shuler, M. L. *Lab Chip* **2005**, *5*, 74−85.
(40) Etame, A. B.; Smith, C. A.; Chan, W. C.; Rutka, J. T. *Nanomedicine* **2011**, *7*, 992−1000.
(41) Xin, H.; Sha, X.; Jiang, X.; Chen, L.; Law, K.; Gu, J.; Chen, Y.; Wang, X.; Fang, X. *Biomaterials* **2012**, *33*, 1673−1681.
(42) Pang, Z.; Gao, H.; Yu, Y.; Chen, J.; Guo, L.; Ren, J.; Wen, Z.; Su, J.; Jiang, X. *Int. J. Pharm.* **2011**, *30*, 284−292.
(43) Hua, M. Y.; Liu, H. L.; Yang, H. W.; Chen, P. Y.; Tsai, R. Y.; Huang, C. Y.; Tseng, I. C.; Lyu, L. A.; Ma, C. C.; Tang, H. J.; Yen, T. C.; Wei, K. C. *Biomaterials* **2011**, *32*, 516−527.
(44) Xie, J.; Lei, C.; Hu, Y.; Gay, G. K.; Bin Jamali, N. H.; Wang, C. H. *Curr. Pharm. Des.* **2010**, *16*, 2331−2340.